AIAA 97-0158
Demodulating Camera System for Picosecond Pump/Probe Imaging

T. Settersten, C. Fisher, N. Middleton
and M. Linne
Division of Engineering
Colorado School of Mines
Golden, Colorado

J. Gord, Wright Laboratory,
Wright Patterson AFB, Ohio

P. Paul and G. Feichtner,
Sandia National Laboratories,
Livermore, California

35th Aerospace Sciences Meeting & Exhibit
January 6-10, 1997 / Reno, NV

DEMODULATING CAMERA SYSTEM FOR PICOSECOND PUMP/PROBE IMAGING

T. Settersten, C. Fisher, N. Middleton and M. Linne
Division of Engineering, Colorado School of Mines, Golden, CO

J. Gord
Wright Laboratories, Wright Patterson AFB, OH

P. Paul and G. Fiechtner
Sandia National Laboratories, Livermore, CA

Abstract

We present further development of an array which is capable of demodulating an image using phase-sensitive detection. Our goal is an imaging system for Pump/Probe, a spatially-resolved, absorption-based diagnostic. The device could also be used for demodulated PLIF, or it could be used with an imaging spectrometer to acquire demodulated cw Raman spectra along a line. Such an imaging system would make it possible to operate at camera framing rates. The most common rate is 30 Hz, but there are architectures which can be driven faster, and in fact these are the arrays we have used in design.

The concept involves demodulation on-chip, using known camera drive techniques. Furthermore, this approach can potentially overcome previous difficulties associated with an optical background. We have developed a model for the concept, used initially to make performance estimates and to begin design of optimum camera control systems. An array developers' kit has been purchased and we are in the process of proving the concept in hardware.

Introduction

Two-dimensional imaging of radical species concentrations in reacting flows (e.g. OH, CH, NO etc.) has yielded a large amount of useful information. As one example, Planar Laser Induced Fluorescence (PLIF)[1] has become the technique of choice for turbulent flame studies. While PLIF has proven invaluable, there are a number of data manipulations required in order to make the measurement quantitative, such as a system calibration and the collisional quenching correction. In non-premixed, turbulent flames it is difficult to quantify the collisional environment within each pixel area in the flow. This has proven to be a significant limitation to the PLIF technique.

We have demonstrated a Pump/Probe diagnostic technique based upon picosecond, mode-locked Ti:sapphire lasers[2]. The principal advantages of this technique include : *i)* Pump/Probe is a spatially resolved absorption-based diagnostic - even species with poor fluorescence yields can be observed; *ii)* the Pump/Probe technique offers a determination of absolute number density, free of corrections and without the need for calibration[3]; *iii)* the high repetition rates of mode-locked lasers (70 - 100 MHz) can make it possible (in single-point) to observe all the time scales of importance in turbulence, or to observe rapid transients (e.g. ignition); and *iv)* picosecond Pump/Probe is not expected to be strongly affected by the collisional environment.

While Pump/Probe offers significant advantages, it is not a background-free technique. With respect to Laser Induced Fluorescence (LIF), Pump/Probe is somewhat more complex to set up and has not been as well proven. LIF is a very well known, simpler approach which is background-free, but is subject to corrections and calibrations. While there are trade-off's to each diagnostic, either one could be used with the camera we describe herein, in order to acquire images. Our principal goal is to develop a camera which can take advantage of the attributes of Pump/Probe. This will require that we overcome the challenge posed by a dc offset problem. If that approach is unsuccessful, the device can be used with LIF to obtain motion pictures with a single laser and camera system.

In what follows, we describe Pump/Probe, demodulation imaging, and present concepts for a system which could be used for demodulation imaging. A camera model which is under development is presented, including our initial performance estimates.

Single-Point Pump/Probe and LIF

In Pump/Probe spectroscopy, the pump beam is

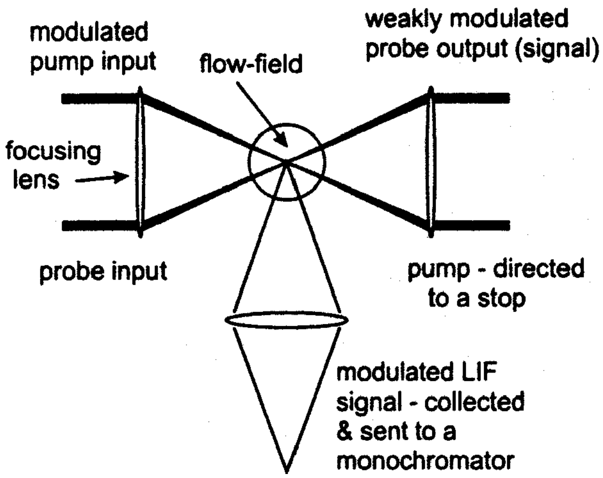

Figure 1. Schematic of single-point Pump/Probe and LIF interaction in the flow-field. In the simplest implementation, both beams are from the same laser.

modulated, and it is crossed with the probe in an absorbing sample (see Fig. 1). The laser is tuned to an absorption line in the molecule of interest. The pump modulation frequency is thus impressed on the resonant molecules via absorption. These molecules then modulate the probe via absorption and stimulated emission. In single-point, the probe modulation is measured with a photodetector and lock-in amplifier (phase sensitive detection), and this measurement can be directly related to the number density of absorbers in the overlap between the two beams. The laser we use is a cw regeneratively mode-locked Ti:sapphire laser pumped with 8 W from a cw Ar:Ion laser. It can be frequency doubled in BBO, and we reliably achieve about 400 mW at 389 nm and at 2 ps pulsewidth.

When the two beams are resonant with the same transition, a model developed by Fiechtner *et al.*[3] shows that the observed modulation depth (α_{MOD}) is related to absolute number density by :

$$\alpha_{MOD} = \frac{g_2}{g_1}\left(1+\frac{g_2}{g_1}\right)\left[\ln\left(\frac{1}{\sqrt{2}-1}\right)\right]^2 \frac{c^4 A_{21}^2 P_{AVE}^{PUMP} N_T L}{16\pi^3 D^2 h \nu_{12}^5 f^L \left(\Delta\nu_{1/2}^L\right)^2} \quad (1)$$

where :

g_i	=	degeneracy of level i = 1 or 2,
D	=	focal diameter,
L	=	beam interaction length,
f^L	=	laser repetition rate,
ν_{12}	=	transition frequency,
$\Delta\nu_{1/2}^L$	=	laser bandwidth,
P_{Ave}^{PUMP}	=	average power of the pump beam,
A_{21}	=	Einstein coefficient for spontaneous emission,
N_T	=	absolute number density of absorber.

Here the modulation resides on a large intensity carrier (typically 10^4 to 10^7 larger than the modulated portion of the signal). The model assumes an optically thin analyte, the linear absorption regime, a 2-level system (OK for Potassium or Calcium), a temporal top-hat pulse profile and broad bandwidth with respect to the absorption linewidth. The modulation depth (α_{MOD}) is easy to measure, and this is related directly to the number density (N_T). The other terms in equation (1) are usually known or can be measured. We demonstrated that Pump/Probe is an absolute determination of number density when this equation was applied to our Potassium measurements and then compared to atomic absorption spectroscopy using a Tungsten filament lamp[2].

Equation (1) is appropriate only for the assumptions listed, but we show it here for simplicity. We have recently developed a model for molecular Pump/Probe interactions, specific to the CH molecule in this case. It is an extension of the model developed by Fiechtner *et al.*[3], relying on many of the same assumptions. We incorporate the various X state, v" = 0 lines overlapping the transform limited line-shape of the laser. The population distributions, linewidths, and individual Einstein coefficients are included. In what follows, several signal estimates for CH are given, and they have been based on this more complex model.

Our proof-of-concept Pump/Probe work was conducted using Potassium (a D line at 766.5 nm) which was seeded into a flame. We have recently set up single-point Pump/Probe measurements using frequency-doubled Ti:sapphire radiation, using Calcium seeded into the same flame (at 422.7 nm). The Calcium experiment was used to determine the lowest modulation depth observable with the current system (on the order of 10^{-5} because we have an unusually noisy pump laser and we are mechanically chopping at 4 kHz). Those experiments indicate that we are limited by the 1/f noise of the laser and the detector. Improvements (laser noise reduction coupled with higher frequency modulation/demodulation, and higher pump power) are under way in order to make a Pump/Probe measurement of CH in a methane/oxygen flame, which is our current goal. For $\alpha_{MOD} = 10^{-5}$ in our current configuration (flame front thickness, pump power, modulation/demodulation frequency, 1/f noise etc.), we estimate a CH detection limit of 10^{16} cm^{-3}, which is a higher concentration than would be found in the welding torch we currently use. This flame limits the interaction length considerably (to less than 100 μm by recent LIF measurements) and it may be necessary to set the system up on a McKenna burner first. As an aside, these issues would be easily overcome by use of a Ti:sapphire amplifier, giving an estimated detection limit of 10^{12} cm^{-3} with no other changes to the system. We have chosen CH as a candidate free radical because the B - X transition overlaps frequency doubled Ti:sapphire. It exists in flames at relatively low concentrations but has a strong Einstein A coefficient.

LIF is a well known technique[4] in which the observed signal is also linearly related to the number density of absorbers. In the linear regime, the signal level is affected by collisional quenching out of the excited state. There are numerous approaches to this quenching problem, one of which is to use a picosecond laser and measure the decay of LIF signal, giving a direct measure of the quenching rate[5]. This technique is limited by the speed of the detection system, but for combustion phenomena slower than the detection system, it is a proven concept.

We typically observe LIF signals whenever we perform Pump/Probe measurements. We have easily observed CH via LIF (with SNR around 1000:1) by passing the collected LIF signal through a monochromator, detecting with a photomultiplier tube (1P28B) and then demodulating with a lock-in amplifier. Because LIF is background-free, the modulated signal is typically small but it competes only with background noise since there is no carrier. Interpretation of the signal is more complex, however, because it is subject to collisional quenching and the collection system must be calibrated. Figure 2 contains one LIF result in which the small methane/oxygen welding torch was scanned through the sample volume to observe CH as a function of position[6]. Similar results have been observed by Renfro *et al.*[7].

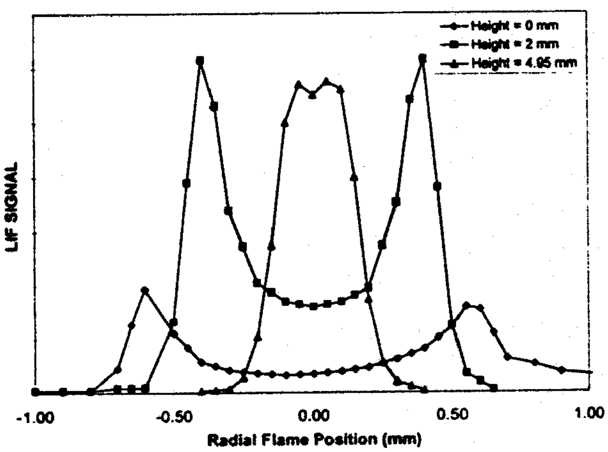

Figure 2. CH LIF signal as a function of position in a methane/oxygen welding torch flame.

Demodulation Imaging

We have demonstrated that Pump/Probe can be used to acquire two-dimensional images of number density in flames[8]. The aspirating burner was used with Potassium, and the laser was operated at 60 ps. The pump beam was expanded into a sheet using cylindrical optics. The probe was then up-collimated into a large diameter, gaussian cross-section beam which intersected the sheet in the flame. It was then necessary to develop a two-dimensional analog to the lock-in amplifier used in the single-point experiments. In our initial demonstration, we used a liquid crystal mounted in front of a normal CCD camera to modulate optical gain (similar to the mixer in a lock-in amplifier). That approach had several problems but it proved sufficient for a proof-of-concept demonstration. Similar ideas have been demonstrated in the field of phase fluorometry for medical imaging. In phase fluorometry, photocathode or image intensifier gain is modulated in front of the camera and this serves as the mixer[9]. The principal difference between the two approaches is that the liquid crystal modulates loss and the image intensifier modulates gain. Both systems suffer from a large dc background problem, and this limits the performance of such camera systems.

In phase sensitive detection, some system input [e.g. the pump beam] is modulated at a known frequency [say at ω_m (rad/sec)]. That system input produces a small modulated signal [in the probe beam]. The modulated signal has the same frequency as the input, but it can have a phase shift and is typically imbedded in a large background consisting of noise components covering a broad range of frequencies [let ω_i represent the various frequency components of the total signal (including the signal modulated at ω_m), see Fig. 3].

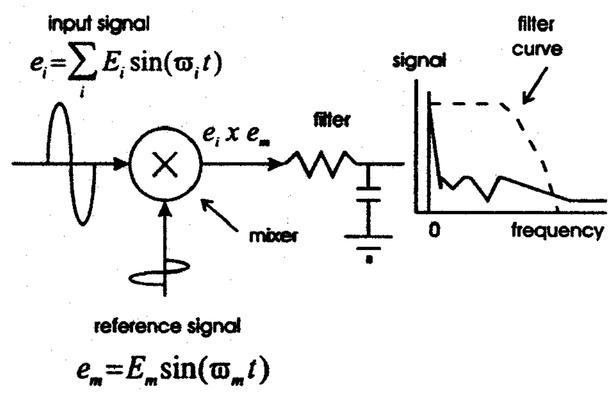

Figure 3. Schematic of the demodulation process.

In a lock-in amplifier, the total signal [modulated signal of interest + large background = $e_i = \Sigma_i E_i \sin(\omega_i t)$] is first demodulated by a mixer. This occurs by multiplication of the total signal $[e_i]$ with a reference sinusoid $[e_m = E_m \sin(\omega_m t)]$ modulated at the chopper frequency ω_m :

$$e_i \times e_m = 0.5\, \Sigma_i (E_i \times E_m)\,[\cos(\omega_i - \omega_m)t - \cos(\omega_i + \omega_m)t] \quad (2)$$

producing sum $(\omega_i + \omega_m)$ and difference $(\omega_i - \omega_m)$ frequency terms for all frequencies of the total signal. The difference term $(\omega_i - \omega_m)$ is at zero frequency only for the modulated signal of interest (since ω_i is the same as ω_m in that specific case). Since $\cos(0) = 1$, the signal of interest is preserved at $\omega = 0$ (dc). In other words, that small portion of the total signal is "mixed down" to dc because it has the same frequency as the original modulator. The output of the mixer is then routed through a low-pass filter which eliminates the sum frequency term of the modulated signal of interest $[\cos(\omega_i + \omega_m)t]$, and any other components (e.g. the large background) which fall outside the bandwidth of the filter. The remainder of the signal carries the information of interest (contained in the sideband which passes through the low-pass filter).

Mixers themselves can be thought of as amplifiers, in which the amplifier gain is modulated at the reference frequency. The amplifier output is the linear product of the input and the gain (now modulated), so this performs the multiplication just described. For imaging, it is possible to accomplish a similar task using optical loss (e.g. by polarization modulation) or gain (e.g. by use of a micro-channel plate or photocathode) directly in front of the camera. It can also be accomplished by clocking photo-electronic charge within the camera architecture, as described below. Filtering can then accomplished by the integrating behavior of the pixel itself, together with the camera framing rate of 30 Hz. This is not necessarily the optimum filter behavior, but it proved sufficient for our first demonstration.

One important difference between two-dimensional, optical phase sensitive detection systems using loss or gain and a lock-in amplifier is that the demodulator is capable of reducing the light level to zero and then driving it up to some maximum level characteristic of the system. The optical signal will not go negative. That can impose a dc offset at the electrical input (see Fig. 4), and hence the product of the reference and signal consists of a large dc level summed with the demodulated signal (the image we care to acquire). The size of this dc offset is a function of the diagnostic technique used. For Pump/Probe, the modulated portion of the signal is carried within a laser beam which is from 10^4 to 10^7 larger. For LIF, the background is caused by flame emission, scattering and noise in the camera.

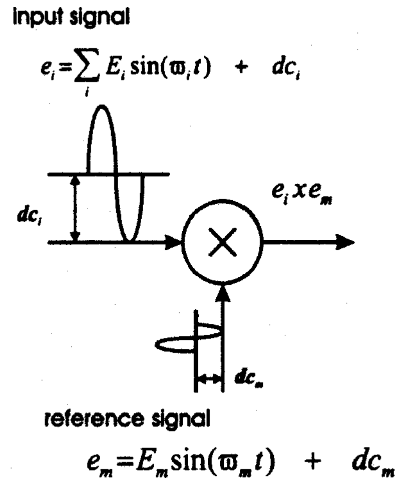

Figure 4. Schematic of optical mixing process.

In frequency space, this offset problem can be described in terms of the reference signal. In a lock-in amplifier, the reference is usually a clean sine wave with no dc offset. That gives spikes at $\pm\omega_m$ in the reference signal frequency spectrum, but the reference signal power at $\omega = 0$ is zero. When the reference is multiplied with the input, the zero at $\omega = 0$ insures that there are no residual components mixed to dc. For optical mixing, however, the reference and input necessarily have a dc offset, since an optical signal can't go negative. That gives spikes at $\pm\omega_m$ in the reference signal frequency spectrum, with large signal power at $\omega = 0$. When optical mixing occurs, the $\omega = 0$ terms are included. One consequence is that when the acquired image is displayed, the dc level (being much larger than the demodulated signal) makes it impossible to observe the demodulated image of interest, even though it is there. It is therefore necessary to find a way to subtract this dc component from the total in order to display the image of interest. It is possible to acquire a dc (without demodulation) image and subtract it from the dc + demodulation image if one is observing a still (or steady) phenomenon[8]. Such an approach is not useful for real-time imaging, however, because dc subtraction in software is too slow. It would be much more beneficial to do this in real-time, at camera framing rates.

This dc offset can also limit the minimum modulation depth detected by the camera, unless we can eliminate it at the sensor. This constitutes an even larger problem for Pump/Probe. The problem can occur in one of two limiting electronic areas. First, digital cameras use capacitive sensors and/or storage areas on-chip. These capacitors have a limit to the charge they can store, given by the specified electron well-depth. In an ideal detector, the minimum modulation depth is then reached when the electron well depth has filled with background (the dc) to the point where the modulated portion of the signal occupies the last two photoelectron sites. In practice, the situation is much worse because electronic and optical noise will fill the a portion of the well, and so the modulated portion must be larger than the noise level by a measurable amount. In a real (e.g. noisy) detector, therefore, the minimum modulation depth is given by (2 x noise)/(total electron well depth). Commercially available cameras are then limited to modulation depths on the order of 10^{-4} to 10^{-5}. This is a useful level of performance, but some applications will need to detect better (smaller) modulation depths. If, following image acquisition in an array, we then transfer the dc+signal to a frame grabber, the analog-to-digital converter will have a modulation depth limitation due to the digitization process itself. As an example, an 8-bit digitizer has a minimum modulation of 1%, much larger than would be useful. For these reasons, we have developed on-chip electronic techniques which both demodulate and remove the dc problem[10].

Our goal then is to develop various optical sensor arrays (linear and 2-D) which demodulate on-chip and which are capable of removing the dc image before or during the time the signals are digitized. There are possible optical solutions to this idea, but it is our belief that electronic solutions will be much more reliable.

2-D Demodulation On-Chip

Here we describe a specific demodulation imaging technique using commercially available hardware and proven charge-clocking techniques. Other approaches may be possible, but they typically require a custom chip. One goal of this work has been to adapt existing hardware, with proven clocking and control signals.

The clock and instruction signals to an interline transfer camera can be modified to perform demodulation. Dereniak and Crowe[11] point out that in an interline transfer camera:

> Vertical readout registers are interlaced with the photosensitive sites, which are arranged in columns. After collecting photoelectrons during some integration time, the charge is transferred to a shielded (aluminum-covered) shift register by a pulse on the transfer gates. The signal charge is now in the column shift registers ... and is clocked out while the next field is being integrated.

This read-out system is unusual. Most commercially available CCD cameras use a frame-transfer architecture, in which the entire acquired image is transferred to a shielded image shift register equivalent in size to the active area of the chip. In effect, an interline transfer camera slices the register into narrow columns placed adjacent to columns of photosensors. Charge shifting is then flexible and fast. Devices like the SONY TCX005 series CCD (as one example) allow one to control the clocking functions, and herein lies the key to this specific idea. Figure 5 contains a diagram of the Sony interline transfer camera architecture. The sensor is a photodiode with positive hole storage layers. After a signal charge has accumulated, the read-out gate transfers the signal charge to the vertical shift register, a capacative storage device.

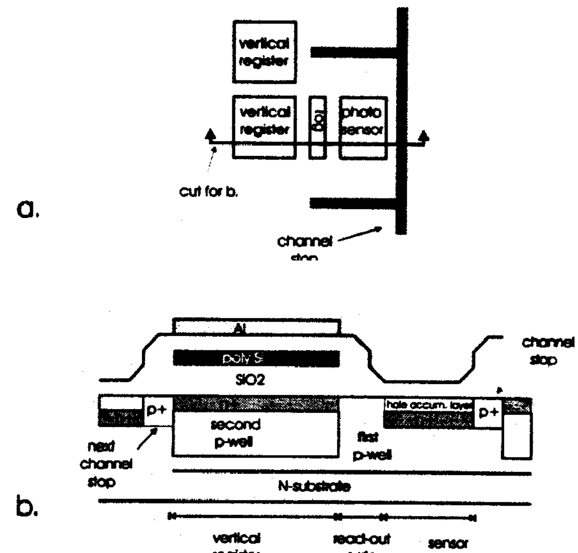

Figure 5. SONY interline transfer architecture, a. top view of chip sector, b. cut-away view.

It is also possible to disable charge storage by transferring charge from the sensor to the substrate. This is a standard command to shutter the camera off. These functions are depicted in the schematic of charge movement in Figure 6. Under normal camera operation, V_3 is the voltage applied to all the gates when reading-out the signal charge from the sensor, while V_1 and V_2 are normally applied to the individual shift register gates for transferring charge along the vertical register; $V_1 < V_2$ (V_2 is more positive). This is the standard "bucket brigade" arrangement for reading out a register. V_{sub} controls the level of the overflow drain. When V_{sub} is low, charge will accumulate in the sensor, but when $V_{sub} = V_{sub} + \Delta V_{sub}$, the sensor charge will dump into the substrate.

Demodulation would involve several charge motion steps. Figure 7 represents a modulated probe signal

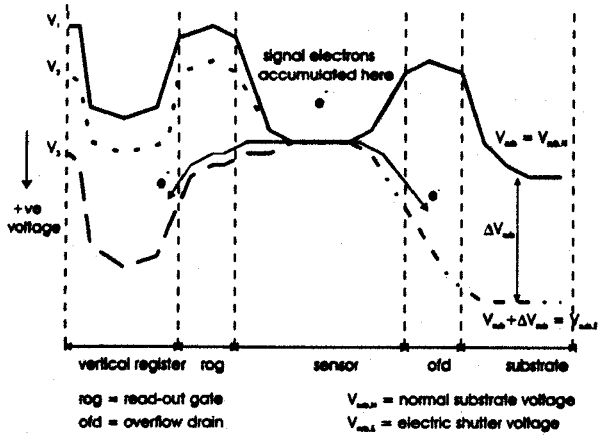

Figure 6. Charge movement in the architecture of Fig. 5.

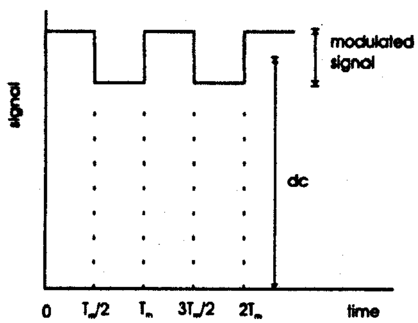

Figure 7. Schematic of modulation and timing. $T_m = 1/f_m$ where f_m is the modulation frequency (Hz).

(where the amplitude of the modulated component is exaggerated and noise components are left off in order to convey the idea). For times less than zero, the gate voltages would be arranged to shutter the camera off, dumping charge into the substrate (see Fig. 8 a.). Next, for times $0 \leq t \leq T_m/2$, the gate voltages would be arranged to store photoelectrons in the shift register (see Fig. 8 b.). Between $T_m/2 \leq t \leq T_m$, the gate voltages would be arranged to shutter the camera off again (Fig. 8 a.). Charge stored in the shift register is not lost in this process. This pattern would be repeated, preferentially storing modulated photoelectrons in the shift register. Sensor gain is then modulated at f_m ($= \omega_m / 2\pi$). For the SONY cameras, f_m can be as large as 100 kHz. This is a somewhat simplified presentation which doesn't account for clocking response time of the camera, as one example, but it serves to explain the idea. Demodulation is then followed by filtering, controlled somewhat by the framing of the storage register and the downstream electronics. We envision using a switched-capacitor filtering.

The signal derived in this fashion contains the dc component described earlier, stored in this case within a capacitor in the vertical register. A simple modification

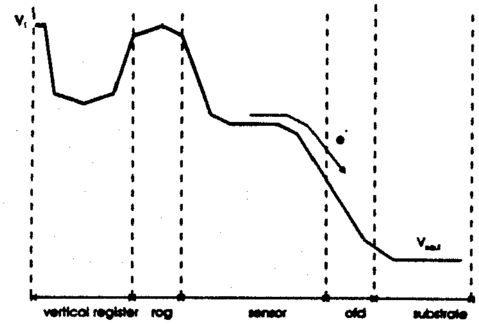

a.

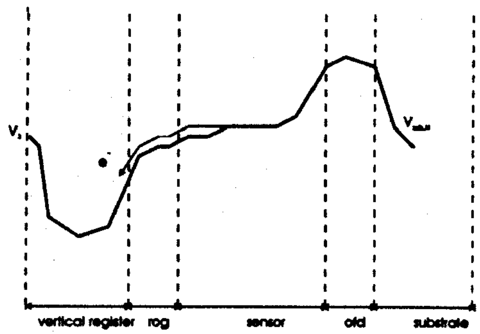

b.

Figure 8. Charge transferring for demodulation : a. $V_{SUB} = V_{SUB,E} = V_{SUB,N} + 23.5$ (V) & $V_1 = 0$; b. $V_{SUB} = V_{SUB,N}$ & $V_3 = 15$ (V).

to the idea just presented, however, could eliminate most of the dc component during the process of demodulation. The anti-blooming servo on some cameras controls the flow of electrons to the register by driving the register voltages to an intermediate point somewhat like V_2 in Figure 6, while leaving $V_{SUB} = V_{SUB,N}$. During times like $0 \leq t \leq T_m/2$, instead of routing all of the charge into the vertical register, the dc level would be trapped by a potential barrier at the read out gate, as depicted in Figure 9. This is analogous to ac coupling, in which the dc level is trapped but the ac portion is passed on. The dc component trapped in the potential barrier would then be dumped into the substrate. Here, the barrier height would be set to pass the largest modulation depth, meaning that some dc would pass with smaller modulation depths, but the overall dc level stored in the register would be significantly reduced. This would allow for the detection of a much smaller modulation depth. This is a fairly new idea, and detailed specifications on the performance of the anti-blooming system have not been found as yet (most camera manufacturers don't make detailed information like this available). It's therefore not possible at this point to speculate on how much of the offset can be handled with this approach, but it clearly could address a large part of the electron well problem.

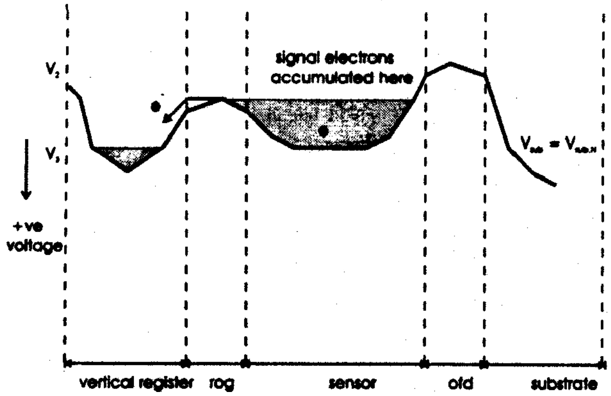

Figure 9. DC subtraction on-chip during demodulation.

The remaining dc background can be subtracted in real time using the architecture depicted in Figure 10. This concept aims to remove residual dc before digitization. Commercially available systems are already manufactured as shown, for color imaging. In that case, the beam splitter is coated with a dielectric which directs certain colors in selective directions. It is a simple change to modify the coating to split the colors into both directions. In practice, the arrays are aligned to each other and mounted on a beam splitter cube. Both CCD's would then demodulate as described, but they would do this 180 degrees out of phase with each other. The two images would then be balanced and subtracted in a difference amplifier before digitization.

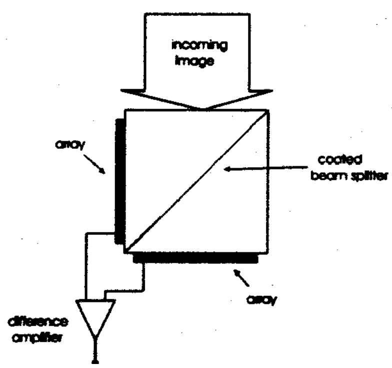

Figure 10. Schematic diagram of matched arrays for dc subtraction.

For very low light levels (for LIF as one example), an image intensifier system [microchannel plate (mcp) and photocathode] could be used. Here, however, the intensifier would be operated dc. An important difference between this technique and the use of an mcp to demodulate is that an mcp produces large relative noise at low voltage levels. Use of the mcp to modulate gain requires that low voltage levels be used at the modulation frequency, increasing noise. Here, we demodulate on-chip and leave the mcp at a fixed voltage, giving significantly less noise. In addition, mcp modulation does not overcome the dc offset problem.

In order to take the next step in camera development, we are pursuing both hardware evaluations and detailed models. With respect to hardware, we are building a mock-up of the camera system just described using discrete components. This system will include three sensors and will be used to evaluate clocking commands, system speed and so on. A second step which is also underway is the modification of a Loral-Fairchild 6,000 element linear array. That device has an architecture very similar to the SONY and Kodak interline transfer CCD's, We plan to develop charge transfer drive systems for this array as a next step in complexity. Finally, we are currently evaluating 2-D arrays and will purchase a developer kit for one of them. In the next section, we discuss device models and give some preliminary performance estimates.

Electronics Model Development

We are currently developing a model for the behavior of the camera system just described. It will be used primarily to evaluate the ability of certain architectures to perform as a demodulator and filter. A large amount of development has gone into modern single-point lock-in amplifiers. It will be necessary for us to deal with the same issues, including minimum modulation depth and dynamic range achievable (a question of architecture and noise), distortion, demodulation frequency, integration time, framing rate, optimization of filtering and digitization. As mentioned above, each of the devices in the chip has a specified transfer function and only a detailed model can indicate whether the system can perform at a reasonable speed. The use of anti-blooming controls to minimize the dc offset is a new idea which has not yet been incorporated into the model, so our current performance estimates are for a more limited device.

A block diagram of the current model, dealing simply with the demodulation step, is shown in Figure 11. We use a block diagram formulation, taking the convolution of transfer functions. The expressions are written and solved first, and then loaded into either MATLAB® or Systemview® (by Elanix), an electronics simulation package. This allows us to evaluate various ideas.

Here we present just one result. In this system of equations, the experimentally observed α_{MOD} is given by $[\, x\, K_S \,/\, (w + x\, K_S)]$. For the case without dc rejection using the anti-blooming servo, we have evaluated the noise level of the camera up to the charge amplifier. We then require the observable modulation depth to be twice that noise level in order to evaluate the minimum

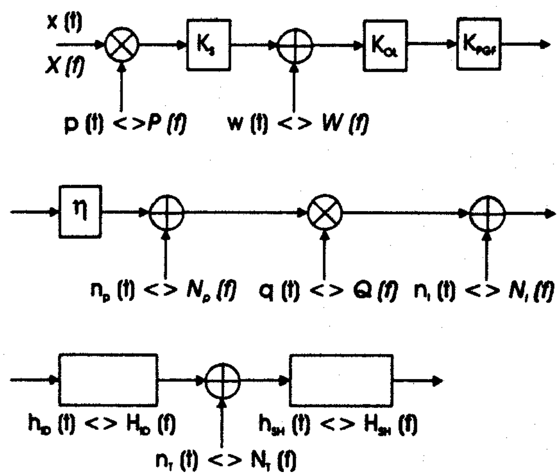

Figure 11. Block diagram of the mixing and amplification process. In the figure :

x = un-modulated Pump/Probe signal,
(t) = time domain functions,
(f) = frequency domain functions,
p = modulation carrier,
K_S = multiplier,
w = background intensity,
K_{OL} = optical losses,
K_{PGF} = pixel geometry factor,
η = quantum efficiency,
n_p = photon shot noise,
q = demodulation reference signal,
n_I = shift register input noise,
H_{ID} = integrate and dump transfer function,
n_T = charge transfer inefficiency noise,
H_{SH} = sample and hold transfer function.

detectable modulation depth. The overall signal noise from sources preceding the amplifier is comprised of photon shot noise, shift register input noise[11] and charge transfer inefficiency noise[11]. In a best-case model, we do not consider the charge amplifier Johnson noise because that occurs after demodulation. Johnson noise does not inhibit demodulation because it does not occupy the electron well. We do not consider noise from the laser source, because at this level of modulation depth the performance of a Pump/Probe system is not limited by laser noise. As a second, worst case evaluation of noise, we use the specified noise level (including Johnson noise) for a similar Kodak camera. For our best-case model, we find that at probe beam power levels on the order of 400 mW, a minimum modulation depth of 1.2×10^{-5} should be possible. Using the specifications for the Kodak camera we find a worst-case estimate of 1.2×10^{-4}. As a reference point, our early single-point Pump/Probe work on Potassium achieved a modulation depth of about 10^{-4}.

One could expect a much better level of performance for the anti-blooming approach. This is true because the modulation depth measured by the camera would now be $\alpha_{MOD} = [\, x\, K_S / (w + w' + x\, K_S)]$, where w' is the summation of dc charge packets held within the potential barrier and then dumped into the substrate. As mentioned above, we have not yet been able characterized what this value is.

A primary goal of this modeling effort is to characterize the temporal performance of the system - the clocking and charge shift behavior. We are currently set up to exercise the model of the camera for the case without dc rejection and will be evaluating the issues listed before (minimum modulation depth and dynamic range achievable etc.). As soon as information on anti-blooming control becomes available, that concept will be added to the model. By testing the discrete component system and the linear array in parallel with modeling, we can calibrate our model and improve our estimates of performance.

Pump/Probe Imaging

Using our molecular Pump/Probe model, we evaluated the following case : 4 cm x 4 cm object field (this is likely a reasonable field size because CH exists in small flame fronts, in ignition kernels for example), use of a 50 kHz amplifier, 2 ps pulse tuned to the R branch of the CH B - X (0,0) band. In order to detect 10^{14} cm^{-3}, the camera would need to detect α_{MOD} around 10^{-6}. Thus, it will be necessary to use dc rejection, via anti-blooming if it proves workable. In order to expand the pump beam into a sheet, it would also be necessary to use a Ti:sapphire amplifier in order to preserve the set of terms :

$$\frac{P_{AVE}^{PUMP}\, L}{LD\, f^{L}}$$

adapted from equation (1). The amplifier output would then form the pump beam, modulated at the amplifier repetition rate. The amplifier requires very little input, so the majority of the oscillator output would form the probe beam. The camera demodulation rate would then be clocked by the amplifier at 50 kHz. At this point the system begins to emulate a 2-D boxcar averager, but phase sensitive detection and boxcar averaging are closely related techniques.

One key attribute of Pump/Probe and Pump/Probe imaging is the pressure insensitivity of the diagnostic. It's worth pointing out that the concentrations we have quoted to this point are for 1 atmosphere. At higher pressures, this diagnostic improves with number density.

Demodulated PLIF Imaging

Demodulated PLIF imaging is a simpler approach. It could be done with a demodulating array which doesn't use any background rejection, since LIF is background free. The camera would require an image intensifier, just as normal PLIF systems do. Based upon our LIF results using fairly low intensities we are confident this could be done. There would be two major differences between this approach and the more normal nanosecond PLIF. First, this system would offer the ability to acquire images at camera framing rates using one laser and one camera. Since we would be controlling clocking functions, the system could be pushed to frame at the highest rate possible within detection constraints. The second principal difference is that nanosecond systems acquire high quality still images frozen in time. Flows faster than our demodulating camera would blur considerably, so it would not be possible to study the same kind of flow. Some flows, however, might lend themselves well to this approach - non-reproducible flame vortex interactions for example[12].

Conclusions

Preliminary work in the area of Pump/Probe imaging indicated that 2-D demodulation could be accomplished, but that for important species determinations it would be necessary to demodulate in a way that removes the dc background problem. After evaluation of various camera architectures and charge clocking systems, we have found an architecture which can demodulate using proven control techniques. In addition, the anti-blooming control appears to be a promising dc rejection idea when used in conjunction with matched arrays. Preliminary modeling indicates that this approach should work and we are developing hardware implementations.

Acknowledgments

This research has been supported by the National Science Foundation through grants CTS-9411391 and DGE-9554559, and by the US Air Force Wright Laboratories through grant number F33615-96-C-2632.

References

1. R.K. Hanson, "Combustion Diagnostics: Planar Imaging Techniques", *Twenty-first Symposium (International) on Combustion/The Combustion Institute*, Pittsburgh, PA, 1677-1691, (1986).
2. G.J. Fiechtner and M.A. Linne, "Absolute Concentrations of Potassium by Picosecond Pump/Probe Absorption in Fluctuating, Atmospheric Flames", Combust. Sci. and Tech., Vol. 100, 11-27, (1994).
3. G.J. Fiechtner, G.B. King, and N.M. Laurendeau, "Rate-equation model for quantitative concentration measurements in flames with picosecond pump-probe absorption spectroscopy", Appl. Opt., Vol. 34, No. 6, 1108-116, (1995).
4. A.C. Eckbreth, *Laser Diagnostics for Combustion Temperature and Species - Second Edition*, Gordon and Breach, Amsterdam, (1996).
5. M.S. Klassen, B.D. Thompson, T.A. Reichardt, G.B. King and N.M. Laurendeau, "Flame Concentration Measurements Using Picosecond Time-resolved Laser Induced Fluorescence", Combust. Sci. and Tech., Vol. 97, 391-403, (1994); T.A. Reichardt, M.S. Klassen, G.B. King and N.M. Laurendeau, "Real-time acquisition of laser-induced fluorescence decays", Appl. Opt., Vol. 34, No. 6, 973-976, (1995).
6. T. Settersten, D. Albers, N. Middletin, M. Linne and P. Paul, "Picosecond Pump/Probe Imaging Systems", Poster No. 222, *Twenty-sixth International Combustion Symposium/The Combustion Institute*, Naples, Italy, (1996).
7. M.W. Renfro, M.S. Klassen, G.B. King and N.M. Laurendeau, "Time-Series Measurements of CH Concentration in Turbulent CH_4/Air Flames Using Picosecond Time-Resolved Laser-Induced Fluorescence", Presented to the Central States Section/the Combustion Institute, (1996).
8. M.A. Linne, D.C. Morse, J.L. Skillowitz, G.J. Fiechtner, and J.R. Gord, "Two-dimensional pump-probe imaging in reacting flows", Opt. Lett., Vol. 20, No. 23, 2414-2416, (1995).
9. see e.g. T.E. French, *The Development of Fluorescence Lifetime Imaging and an Application to Immunology*, Ph.D. Thesis, Department of Physics, University of Illinois at Urbana-Champaign, (1996)., and the references found therein.
10. M. Linne, N. Middleton, D. Morse, C. Fisher, and P. Paul, *A Synchronously Demodulating Camera*, Patent application, (1996).
11 E.L. Dereniack, and D.G. Crowe, *Optical Radiation Detectors*, John Wiley & Sons, New York, (1984).
12. J. Hertzberg, J. Carlton, M. Schweiterman, E. Bradley and M. Linne , "Splitting of an Axially Excited Jet Diffusion Flame", Presented at the 1996 International Mechanical Engineering Congress and Exposition, Atlanta, GA, Nov 17-22, (1996).